Connected Slot Antennas for Wideband Wide-Scan Phased Arrays

Cavallo, Daniele

DOI
10.1109/ARRAY58370.2024.10880312

Publication date
2024

Document Version
Final published version

Published in
2024 IEEE International Symposium on Phased Array Systems and Technology, ARRAY 2024

Connected Slot Antennas for Wideband Wide-Scan Phased Arrays

Daniele Cavallo
Microelectronics dept.
Delft University of Technology
Delft, Netherlands
d.cavallo@tudelft.nl

***Abstract*—A review on wideband wide-scanning arrays based on connected slot elements with artificial dielectric superstrates is given. The analysis method to evaluate the active input impedance of the unit cell is described and its application to wideband array designs is discussed. Design examples reaching up to 10:1 bandwidth are presented, including experimental results from prototypes. The typical achieved performance is compared with the state-of-the-art. Aspects such as cross-polarization levels and finite edge effects are also discussed.**

Keywords—artificial dielectrics, connected arrays, spectral domain method, wideband arrays

I. Introduction

Wideband wide-scanning arrays have become a popular research topic in the field of phased array antennas, because of their favorable use in multifunction antenna systems. When limited space is available on complex platforms, an ultra-wideband antenna aperture combining several functions is desirable. Although being traditionally employed primarily for radar [1] and radio-astronomy applications [2], recently broadband arrays are gaining interest also for satellite and mobile communications [3], [4], also due to the technological advancement of low-cost transmit/receive (T/R) modules [5].

Existing wideband array concepts include tapered slot or Vivaldi antennas [6], [7], bunny-ear elements [8], [9], tightly coupled arrays [10]–[12], connected arrays [13]–[16]. This last family of wideband arrays is particularly advantageous because of its low-profile and planar structure, and because it is amenable to efficient analytical modeling. More specifically, the active input impedance of a connected array unit cell embedded in a known stratified medium can be written in closed form [14]. The stratification can include dielectric slabs or metal layers that can be described by an equivalent impedance. These models allow simulating the unit cell with negligible computational resources, enabling the optimization of the design.

A specific implementation of connected arrays is based on connected slot elements loaded with artificial dielectric layers [17], [18]. Artificial dielectric layers (ADLs) are periodic arrangements of sub-wavelength metal patches to synthesize a desired effective refractive index. Unlike conventional dielectric slabs, ADLs are strongly anisotropic and do no support surface waves, enabling wide scan performance. Moreover, they allow to overcome the frequency dependence of the reflector and to enlarge the bandwidth.

An overview of the different ongoing research activities in the field of connected arrays with ADLs will be given, including analysis, modelling, and design aspects. Feeding strategies for the unit cell, as well as methods to reduce the cross-polarization levels and considerations on the finite edge effects will be also presented at the conference.

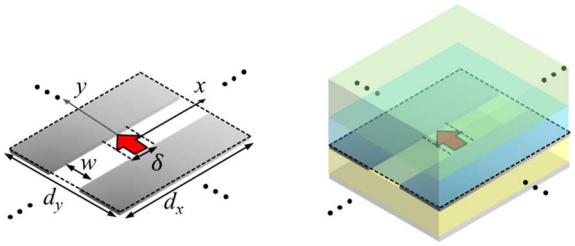

(a) (b)

Fig. 1. (a) Connected slot unit cell with characteristic parameters and (b) same unit cell embedded in a generic planar stratification.

II. Unit Cell Analysis

A. Active Input Impedance

A general connected array unit cell is depicted in Fig. 1(a) and consists of an *x*-oriented connected slot element, with periods d_x and d_y along *x* and *y*, respectively. The slot width is indicated by *w*, and δ refers to the delta-gap feed size. The slot is located within a general stratified dielectric medium, as shown in Fig. 1(b). One can write the input impedance of such a unit cell as a Floquet sum [19]:

$$Z_{\text{in}} = -\frac{1}{d_x}\sum_{m_x=-\infty}^{\infty}\frac{\text{sinc}^2\left(\frac{k_{xm}\delta}{2}\right)}{D(k_{xm})} \tag{1}$$

where the Floquet wavenumber with index m_x is $k_{xm} = k_{x0} - 2\pi m_x/d_x$, $k_{x0} = k_0\sin\theta\cos\phi$, θ and ϕ are the zenith and azimuthal scan angles in free space, respectively, and k_0 is the free-space wavenumber. The function $D(k_{xm})$ depends on the given stratification above and below the slot and can be found as:

$$D(k_{xm}) = \frac{1}{d_y}\sum_{m_y=-\infty}^{\infty} G_{xx}^{hm}(k_{xm}, k_{ym})\, J_0\left(\frac{k_{ym}w}{2}\right) \tag{2}$$

where G_{xx}^{hm} is the xx-component of the spectral dyadic Green's function of the stratified dielectric media above and below the slots, with $k_{ym} = k_{y0} - 2\pi m_y/d_y$ and $k_{y0} = k_0\sin\theta\sin\phi$. The zero-th order Bessel function is the Fourier transform of the transverse distribution of the magnetic current in the slot, which is assumed to be edge singular.

The typical stratification that we consider in realistic designs is the one in Fig. 2(a), for which the slot is placed on a grounded dielectric slab as substrate, while ADLs are used as superstrate. The Green's function G_{xx}^{hm} can be found by solving for the current and voltage in the equivalent transmission lines shown in Fig. 2(b), for transverse electric (TE) and transverse magnetic modes (TM), respectively. One of the key aspects of this method is the accurate estimation of the equivalent shunt impedances of the ADLs to be placed in the transmission lines ($Z_{i\text{TE}}$ and $Z_{i\text{TM}}$ for the *i*th layer).

2024 IEEE International Symposium on Phased Array Systems and Technology (ARRAY) | 979-8-3503-9214-2/24/$31.00 ©2024 IEEE | DOI: 10.1109/ARRAY58370.2024.10880312

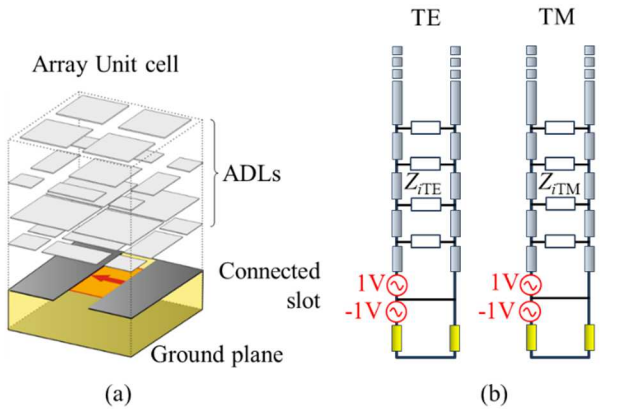

Fig. 2. (a) Connected slot unit cell with ADL supestrate and (b) equivalent transmission lines to calculate the spectral Green's function.

These impedances are known in closed form for non-periodic layers embedded in a homogeneous medium [20]. However, when dielectric and bonding layers are included in the ADLs for realistic implementations, the formulas for the equivalent impedance have to be corrected to account for the change in the effective layer permittivity. Our latest efforts in ADL modeling are oriented in the generalization of the equivalent impedance formulas to accurately account for the complex dielectric stratification in which ADLs are embedded.

III. Design Examples

The model of the unit cell given in Sec. II provides with negligible computation time the active input impedance of the array. The ADLs is first synthesized to implement a desired impedance transformer. The equivalent circuit of ADLs in Fig. 2(b) provides almost instantaneously the geometrical parameters of each layer of the ADLs to match a certain frequency response, obtained by simple impedance transformer theory [21]. The resulting ADLs is then combined with the slot and the backing reflector, to constitute the input starting geometry for an optimization algorithm that minimizes for example the active reflection coefficient for different scanning conditions and over a target bandwidth.

Based on the described procedure, several designs have been demonstrated. For example, a 4:1 band array was recently presented in [15], consisting in a dual-polarized array with 8-layer ADL. The prototype and the measured active voltage standing wave ratio (VSWR) are shown in Fig. 3, compared with simulations.

The concept can be also extended to wider bandwidths, by increasing the electrical height and the number of layers in the ADL superstrate. As an example, the unit cell shown in Fig. 4 can cover a 10:1 bandwidth, by including 12 layers.

The model in Fig. 2 only considers ideal delta-gap sources located on the slot plane. However, realistic feeds can be realized with microstrip and integrated coaxial lines, or with pin-fed parallel plate waveguides. Details on the design of feeding structures will be given at the conference.

IV. Conclusions

Connected slot arrays with artificial dielectric superstrates constitute a valid solution for ultra-wideband array designs. One of the main advantages of this concept is that it is amenable to a simple and accurate analytical description of the unit cell, which allows for automatic optimizations of the performance. Some design examples were shown for bands up to 10:1 and 60° maximum scan angle for every azimuth.

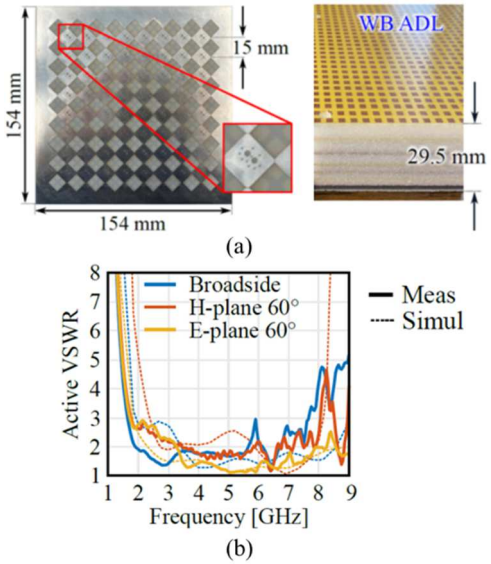

Fig. 3. (a) 2-8 GHz connected prototype and (b) measured active VSWR.

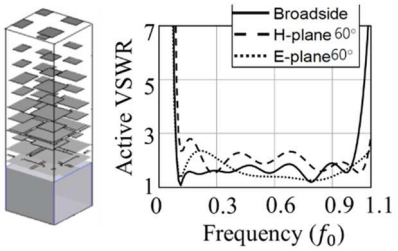

Fig. 4. Example of unit cell design with 12 layers ADL and a 10:1 bandwdith.

References

[1] S. Kemkemian and M. Nouvel-Fiani, "Toward common radar and EW multifunction active arrays," in *Proc. IEEE Int. Symp. Phased Array Syst. Tech.*, 2010, pp. 777-784.

[2] D. H. Schaubert, A. O. Boryssenko, A. Van Ardenne, J. G. Bij de Vaate, and C. Craeye, "The square kilometer array (SKA) antenna," in *Proc. IEEE Int. Symp. Phased Array Syst. Technol.*, Oct. 14-17, 2003, pp. 351-358.

[3] A. J. van Katwijk, A. Neto, G. Toso, and D. Cavallo, "Design of wideband wide-scanning dual-polarized phased array covering simultaneously both the Ku- and the Ka-satcom bands," in *Proc. 14th Eur. Conf. Antennas Propag.*, Mar. 2020, pp. 1-3.

[4] M. H. Novak, F. A. Miranda, and J. L. Volakis, "Ultra-wideband phased array for millimeter-wave ISM and 5G bands, realized in PCB," *IEEE Trans. Antennas Propag.*, vol. 66, no. 12, pp. 6930-6938, Dec. 2018.

[5] G. Amendola et al., "Low-earth orbit user segment in the Ku and Ka band: An overview of antennas and RF front-end technologies," *IEEE Microw. Mag.*, vol. 24, no. 2, pp. 32-48, Feb. 2023.

[6] R. Kindt and R. Pickles, "12-to-1 bandwidth all-metal Vivaldi array element," *IEEE Antennas Propag. Soc. Int. Symp.*, North Charleston, SC, USA, 2009, pp. 1-4.

[7] R. W. Kindt and J. T. Logan, "Dual-polarized metal-flare sliced notch antenna array," *IEEE Trans. Antennas Propag.*, vol. 68, no. 4, pp. 2666-2674, Apr. 2020.

[8] J. J. Lee and S. Livingston, "Wide band bunny-ear radiating element," *Proc. of IEEE Antennas and Propag. Soc. Int. Symp.*, Ann Arbor, MI, USA, 1993, pp. 1604-1607, vol. 3.

[9] M. W. Elsallal and J. C. Mather, "An ultra-thin, decade (10:1) bandwidth, modular "BAVA" array with low cross-polarization," *IEEE Int. Symp. Antennas and Propag.*, Spokane, WA, USA, 2011, pp. 1980-1983.

[10] J. T. Logan, R. W. Kindt, M. Y. Lee and M. N. Vouvakis, "A new class of planar ultrawideband modular antenna arrays with improved

bandwidth," *IEEE Trans. Antennas Propag.*, vol. 66, no. 2, pp. 692-701, Feb. 2018.

[11] J. P. Doane, K. Sertel, and J. L. Volakis, "A wideband, wide scanning tightly coupled dipole array with integrated balun (TCDA-IB)," *IEEE Trans. Antennas Propag.*, vol. 61, no. 9, pp. 4538-4548, Sep. 2013.

[12] E. Yetisir, N. Ghalichechian, and J. L. Volakis, "Ultrawideband array with 70° scanning using FSS superstrate," *IEEE Trans. Antennas Propag.*, vol. 64, no. 10, pp. 4256-4265, Oct. 2016.

[13] J. J. Lee, S. Livingston, and D. Nagata, "A low profile 10:1 (200-2000 MHz) wide band long slot array," *Proc. IEEE Antennas and Propag. Soc. Int. Symp.*, San Diego, CA, Jul. 5-11, 2008.

[14] W. H. Syed, D. Cavallo, H. T. Shivamurthy, and A. Neto, "Wideband, wide-scan planar array of connected slots loaded with artificial dielectric superstrates," *IEEE Trans. Antennas Propag.*, vol. 64, no. 2, pp. 543-553, Feb. 2016.

[15] R. Ozzola, A. Neto, U. Imberg and D. Cavallo, "Connected slot array with interchangeable ADL radome for Sub-8 GHz 5G applications," *IEEE Trans. Antennas Propag.*, vol. 72, no. 1, pp. 992-997, Jan. 2024.

[16] Y. Li, S. Xiao, and B. Wang, "A wideband circularly polarized connected parallel slot array in the presence of a backing reflector," *IEEE Access*, vol. 8, pp. 26517-26523, 2020.

[17] M. Cooley et al., "Planar-fed folded notch (PFFN) arrays: A novel wideband technology for multi-function active electronically scanning arrays (AESAs)," *IEEE Int. Symp. Phased Array Systems Tech.*, Waltham, MA, USA, 2016, pp. 1-6.

[18] D. Cavallo, "Recent advances on wideband wide scanning connected slot arrays," *IEEE Int. Symp. Phased Array Systems & Tech.*, Waltham, MA, USA, 2022, pp. 1-3.

[19] A. Neto and J. J. Lee, "Ultrawide-band properties of long slot arrays," *IEEE Trans. Antennas Propag.*, vol. 54, no. 2, pp 434-543, Nov. 2006.

[20] D. Cavallo and R. M. van Schelven, "Closed-form analysis of artificial dielectric layers with non-periodic characteristics," in *Proc. Eur. Conf. Antennas Propag.*, Krakow, Poland, Apr. 2019, pp. 1-5.

[21] D. M. Pozar, *Microwave Engineering, 4th Ed.* Hoboken, NJ: John Wiley & Sons, Inc., 2012.